Science Advances
AAAS

advances.sciencemag.org/cgi/content/full/5/2/eaav3274/DC1

Supplementary Materials for

Slow slip events in the roots of the San Andreas fault

Baptiste Rousset*, Roland Bürgmann, Michel Campillo

*Corresponding author. Email: rousset@berkeley.edu

Published 13 February 2019, *Sci. Adv.* **5**, eaav3274 (2019)
DOI: 10.1126/sciadv.aav3274

This PDF file includes:

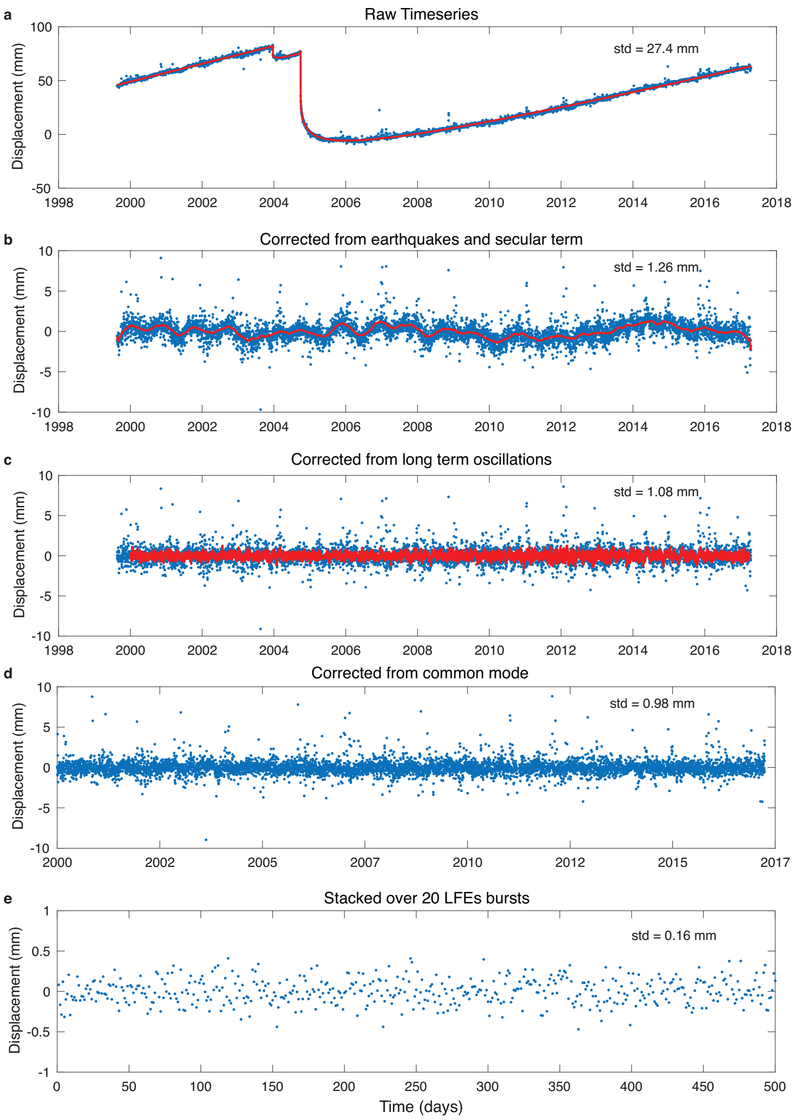

Fig. S1. GPS postprocessing. Example of the GPS processing for the station CAND, north component. Blue correspond to the residual GPS time series and red to the different models for specific corrections. (a) Raw GPS time series, modeled as, $x(t)$, a sum of coseismic steps, postseismic relaxations and a secular term. (b) Long-term oscillations fitted by a 150-day moving average window, $l(t)$. (c) Common mode, $c(t)$, modeled by the first component of a probabilistic principal component analysis . (d) Residual time series after all the corrections. (e) 500-day time series stacked over 20 bursts of LFEs. Note the standard deviation reduction at each step.

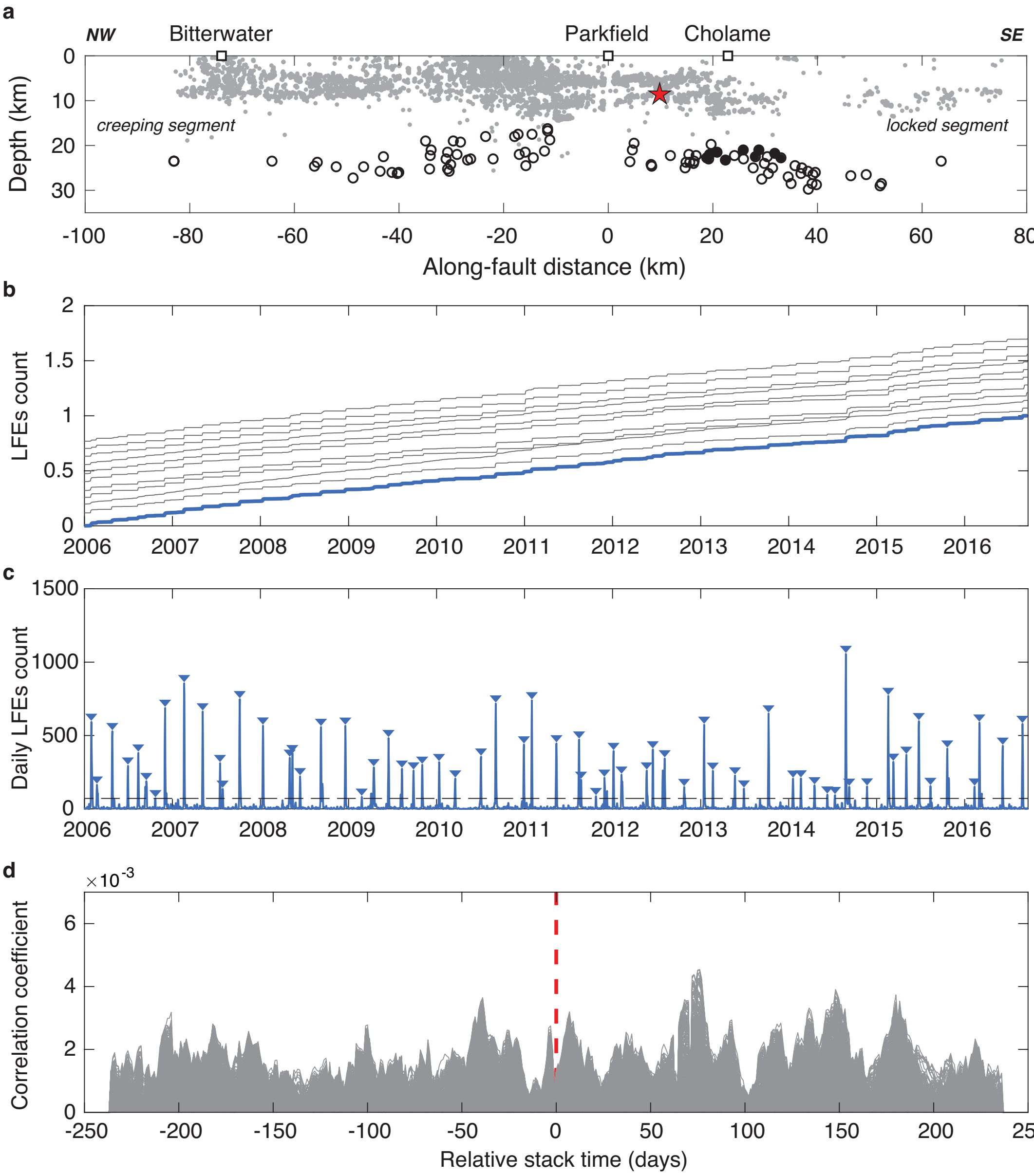

Fig. S2. Correlation analysis for the Cholame segment. (a-c) similar to Figure 2, but for the Cholame LFEs episodic families shown by the filled black circles in (a). The detection threshold is set at 70 daily LFEs (dashed black line in c). (d) Similar to Figure 3a, but using the timing of the Cholame LFE bursts shown by the triangles in c.

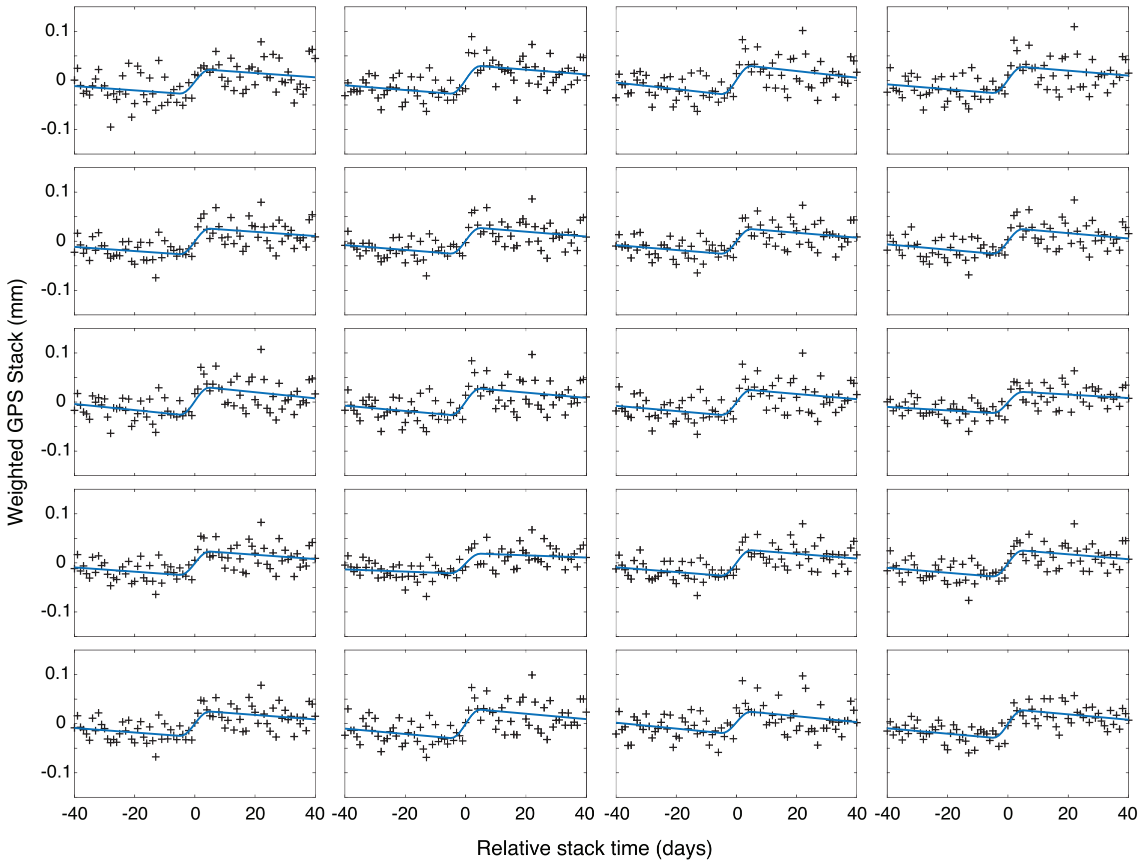

Fig. S3. Jackknife tests with one event removed. Weighted stacks of GPS time series for the jackknife test. On each of the subplots, one transient event has been removed to compute the stack. The blue curves present the best models using a 10-day transient plus a linear term. The transient modeled offsets on these subplots are used to estimate the M_w histogram presented in Figure 4b.

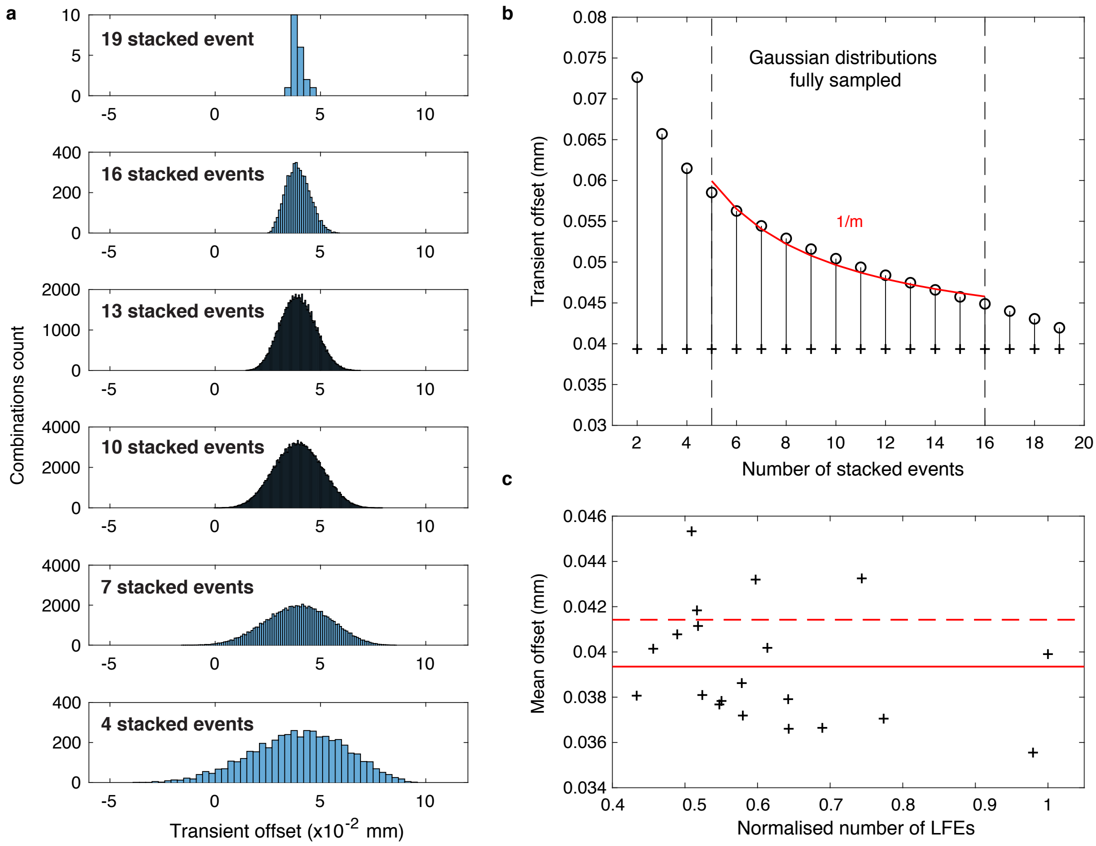

Fig. S4. Jackknife tests. Distribution of the transient offsets for different combinations of events. (a) Distributions of the transient offsets for all possible combinations while removing 1, 4, 7, 10, 13, and 16 events from 20 events. (b) Mean (crosses) and standard deviation (circles) for the distributions with 1 to 19 stacked events ($m = 2$ to $m = 19$, with $n = 20$). The red line presents a 1/m least-squares fit, where m is the number of stacked events. The dashed lines show the limits of the fully sampled Gaussian distributions. (c) Mean offsets for $n = 19$ as a function of the normalised number of LFEs per burst. The red line shows the mean offset for $n = 20$ and the dashed red line the expected offset mean for $n = 19$, in the case of a removed event with zero offset.

Since high-precision borehole strainmeters are installed close to Parkfield, we looked for a signal related to the SSEs detected by GPS in the recordings of these instruments. The forward model of the average transient event detected by the GPS analysis predicts transient with amplitudes on the order of 10 nanostrains for the differential extension and engineering shear strains at the boreholes B073, B075 and B076 (fig. S5). Despite correcting for offsets, tidal strains, barometric pressure variations, and long-term borehole trends, the strain time series still present fluctuations with amplitudes higher than the signal we are looking for at periods of about a week, preventing any clear characterization. Stacking strain time series windows over several events or stations is not improving the signal to noise ratio because the stack is always dominated by the higher amplitude fluctuation, which in most cases is a noise fluctuation. This is mainly due to the fact that the noise level varies at different boreholes and even at different gauges of a single borehole [48].

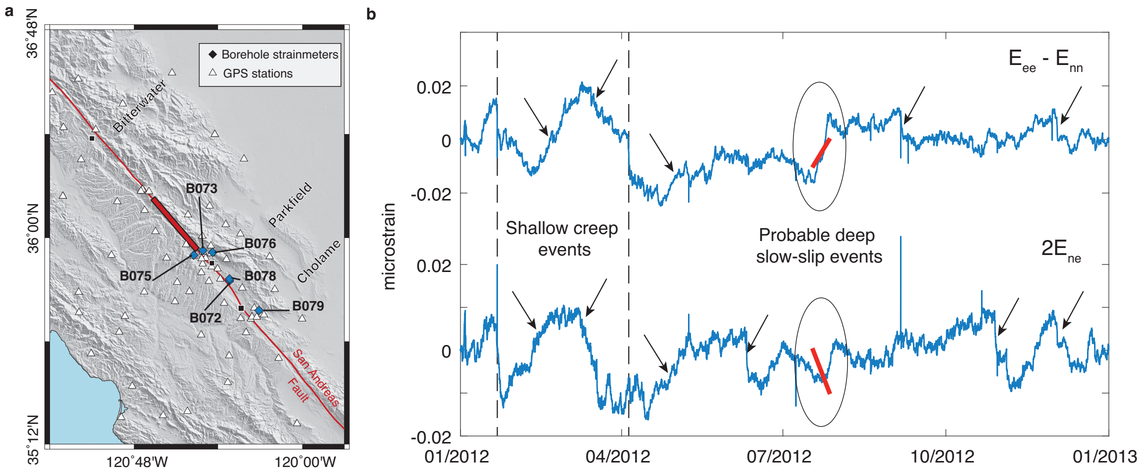

Fig. S5. Strainmeter time series analysis. (a) Map showing the location of the Parkfield borehole strainmeters (blue diamonds). The surface projection of the patch used to compute the forward strain model is shown by the thick red bar. The GPS stations are shown by the white triangles and the cities by black squares. (b) Example of post-processed strain time series at the borehole B073 and for the year 2012. The top time series presents the differential extension strain and the bottom time series is the engineering shear strain. Offsets, tidal strain, barometric pressure and borehole long-term trends have been corrected. The dashed lines indicate the times of short-term ($\sim$ 1 hour) well characterized shallow creep events [49]. The red lines show the strain due to a 10-day M_w 4.9 transient event located on the patch shown in (a), at time of a LFE surge used in the GPS analysis. The black arrows highlight different $\sim$ 10-day or longer excursions in the time series of unknown origin and with higher amplitude than the signal we are searching for, preventing any interpretation of the strainmeter transient signal.

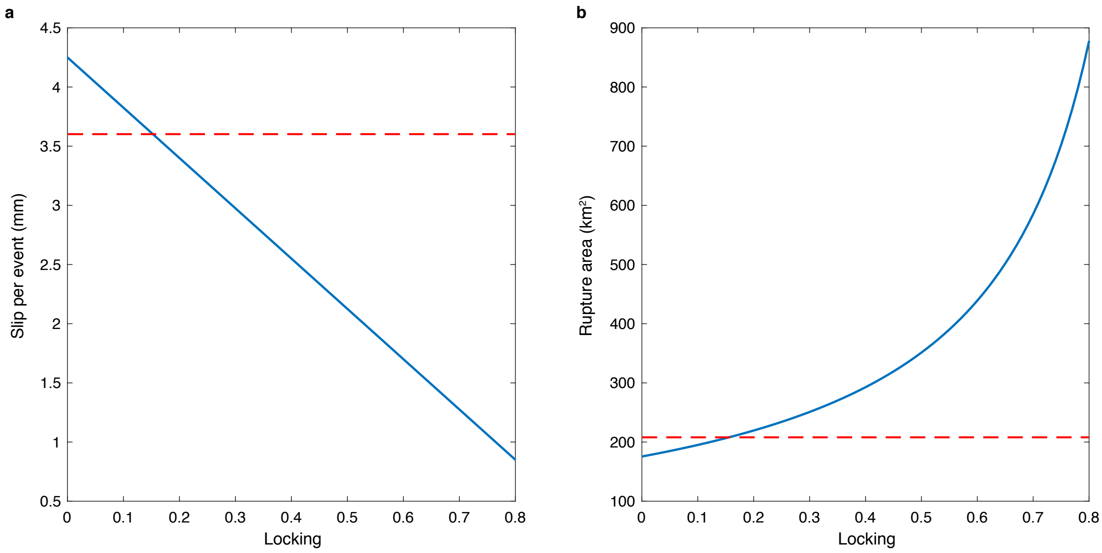

Fig. S6. LFEs as creepmeters. Slip and rupture areas as a function of fault locking. This figure assumes that LFEs are reliable creepmeters, i.e. 25 % of the interseismic aseismic slip is occurring during the slow slip events. With this assumption, only one combination of slip per event (a) and rupture area (b) for a given locking fraction can produce M_w 4.9 events. The dashed red line in (b) is the rupture area shown by the black rectangle in Fig. 3c. The corresponding slip per event is the dashed red line in (a).